

## REVIEW ARTICLE



## Antidepressants enter cells, organelles, and membranes

Zack Blumenfeld<sup>1,2</sup>, Kallol Bera<sup>3</sup>, Eero Castrén<sup>4</sup> and Henry A. Lester<sup>1</sup>✉

© The Author(s), under exclusive licence to American College of Neuropsychopharmacology 2023

We begin by summarizing several examples of antidepressants whose therapeutic actions begin when they encounter their targets in the cytoplasm or in the lumen of an organelle. These actions contrast with the prevailing view that most neuropharmacological actions begin when drugs engage their therapeutic targets at extracellular binding sites of plasma membrane targets—ion channels, receptors, and transporters. We review the chemical, pharmacokinetic, and pharmacodynamic principles underlying the movements of drugs into subcellular compartments. We note the relationship between protonation-deprotonation events and membrane permeation of antidepressant drugs. The key properties relate to charge and hydrophobicity/lipid solubility, summarized by the parameters LogP,  $pK_a$ , and  $\text{LogD}_{\text{pH}7.4}$ . The classical metric, volume of distribution ( $V_d$ ), is unusually large for some antidepressants and has both supracellular and subcellular components. A table gathers structures, LogP,  $pK_a$ ,  $\text{LogD}_{\text{pH}7.4}$ , and  $V_d$  data and/or calculations for most antidepressants and antidepressant candidates. The subcellular components, which can now be measured in some cases, are dominated by membrane binding and by trapping in the lumen of acidic organelles. For common antidepressants, such as selective serotonin reuptake inhibitors (SSRIs) and serotonin/norepinephrine reuptake inhibitors (SNRIs), the target is assumed to be the eponymous reuptake transporter(s), although in fact the compartment of target engagement is unknown. We review special aspects of the pharmacokinetics of ketamine, ketamine metabolites, and other rapidly acting antidepressants (RAADs) including methoxetamine and scopolamine, psychedelics, and neurosteroids. Therefore, the reader can assess properties that markedly affect a drug's ability to enter or cross membranes—and therefore, to interact with target sites that face the cytoplasm, the lumen of organelles, or a membrane. In the current literature, mechanisms involving intracellular targets are termed “location-biased actions” or “inside-out pharmacology”. Hopefully, these general terms will eventually acquire additional mechanistic details.

*Neuropsychopharmacology*; <https://doi.org/10.1038/s41386-023-01725-x>

## INTRODUCTION

Since the early 20th Century, neuropharmacology has advanced in large part by studying interactions between drugs and the extracellular binding sites of plasma membrane (PM) targets—ion channels, receptors, and transporters. Such interactions initiate many canonical pathways leading to downstream intracellular cascades. Antidepressants are among the most crucial and least understood neuropharmacological agents, and they comprise classes of compounds ranging from the Li ion ( $\text{Li}^+$ ) to anesthetic agents to neurosteroids. Although most researchers assume that each class of antidepressant has its own mechanism, for no compound has the mechanism(s) been described satisfactorily; but the often-unstated overarching framework has been extracellular binding.

In fact, several classes of antidepressant drug are known to encounter their targets inside cells. This Introduction provides two early examples, then two more recent examples. We also summarize analogous events with two abused drug classes. Later sections of this review describe the biophysical principles of drug permeation.

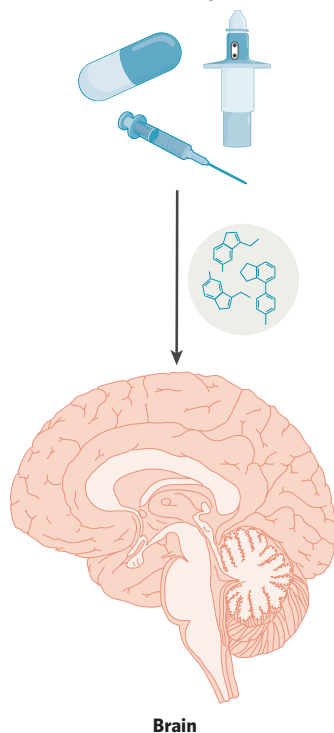
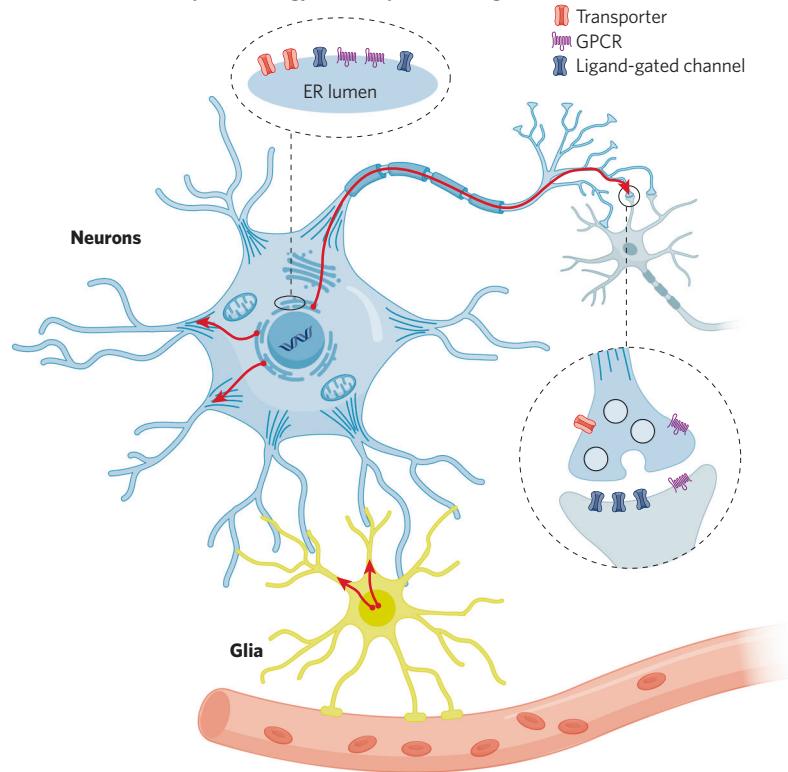
1. Both the A and B subtypes of monoamine oxidase, the eponymous target of MAO inhibitors, exist primarily in the mitochondrial outer membrane of neurons and glia [1–3].

2.  $\text{Li}^+$  was introduced for bipolar disorder in 1949, when the disorder still bore the adjective “manic-depressive” [4].  $\text{Li}^+$  acts primarily as a mood stabilizer. Although  $\text{Li}^+$  is probably an important trace element,  $\text{Li}^+$  has few known extracellular binding sites, and most theories of mood stabilization by  $\text{Li}^+$  assume intracellular binding site(s) [5].  $\text{Li}^+$  enters cells primarily via channels and transporters that physiologically transport  $\text{Na}^+$ , which lies immediately above  $\text{Li}^+$  in the periodic table [5]. This route of entry differs from that used by most the drugs reviewed here, which enter the cytosol via passive permeation through membranes.
3. Two recent studies showed that while the  $5\text{HT}_{2A}$  receptors on the plasma membrane mediate the hallucinogenic effects of psychedelic compounds, their plasticity-promoting effects are mediated by other receptors [6, 7]. The evidence in these studies will be summarized below. In brief, one study showed that the plasticity-inducing effects are caused by intracellular  $5\text{HT}_{2A}$  receptors [6]; the other, that their plasticity-promoting and antidepressant effects are mediated by membrane-spanning regions of TrkB [6, 7]. Perhaps the plasticity effects, which may be correlated with antidepressant effects, represent reopening of a critical period [8].

<sup>1</sup>Division of Biology and Biological Engineering, California Institute of Technology, Pasadena, CA, USA. <sup>2</sup>Keck School of Medicine of the University of Southern California, Los Angeles, CA, USA. <sup>3</sup>Department of Neurosciences and Howard Hughes Medical Institute, University of California at San Diego, La Jolla, CA, USA. <sup>4</sup>Neuroscience Center, University of Helsinki, Helsinki, Finland. ✉email: [lester@caltech.edu](mailto:lester@caltech.edu)

Received: 12 June 2023 Revised: 28 August 2023 Accepted: 28 August 2023

Published online: 02 October 2023

**a Various forms of antidepressant treatment****b “Inside-out” neuropharmacology of antidepressant drugs**

**Fig. 1** **A cellular-level “inside-out” view of antidepressant actions.** **a** Antidepressants can be administered orally, by injection, or by inhalation. **b** Antidepressants pass the blood-brain barrier and enter the CSF. Antidepressants enter neurons or glia via mechanisms described in the text. Some antidepressants also enter organelles and membranes. “Inside-out” hypotheses [13] emphasize entry into the lumen of vesicles in the early exocytotic pathway, such as the ER and the Golgi apparatus. There, antidepressants may encounter their nascent classical targets such as receptors, ion channels, and transporters. The resulting non-classical mechanisms include “pharmacological chaperoning” of the targets, “matchmaking” between the targets and other macromolecules, “abduction” of the targets away from the physiological destinations, “escorting” to non-classical destinations, and modified stress pathways. The altered molecules and low-MW signals that result from “inside-out” pathways may eventually reach the nucleus to change gene activation, the plasma membrane to change excitability, and other cells to change circuit properties. Additional “inside-out” pathways would include inhibition of activation of intracellular enzymes, activation or inhibition of classical G protein signaling within organelles, actions of drug metabolites, and other events discussed in this volume.

4. Another recent report invoked the longstanding observation that the intracellular PDZ-binding domain of neuronal nitric oxide synthase governs its interaction with SERT. The interaction influences signaling by serotonin. This interaction was decreased by use of a membrane-permeant dipeptide, which showed activity in rodent models of antidepressant action [9].
5. Two classes of abused drugs bind to their classical binding sites not only on the PM but also intracellularly. (5a) Nicotine activates PM  $\alpha 4\beta 2$  nicotinic acetylcholine receptors (nAChRs), a class of ligand-gated channels. Nicotine also permeates into the endoplasmic reticulum (ER), where it serves as a pharmacological chaperone for nascent  $\alpha 4\beta 2$  nAChRs. The resulting upregulation of  $\alpha 4\beta 2$  nAChRs plays a large role in the early events—days to weeks—of nicotine dependence [10].

(5b)  $\mu$ -opioid agonists activate the plasma membrane G protein-coupled  $\mu$ -opioid receptor (MOR). Low-molecular-weight (MW) agonists (but not the endogenous peptide agonists) also permeate into recycling endosomes and the distal Golgi, where they continue to activate MOR [11] and may also enhance endocytosis of MOR. The latter process plays a large role in tolerance to  $\mu$ -opioids [12].

Examples (1) through (5) above instantiate some concepts of intracellular binding in psychiatry; and (1) through (4) have direct relevance to antidepressants. Here, we review the mechanisms by which nearly all antidepressants enter cells, their membranes, and their organelles. We emphasize rapidly acting antidepressants

(RAADs), but we review antidepressants now approved for clinical use as well as candidate antidepressants that showed efficacy in preclinical models. Terms such as “localization-biased signaling” [11] and “inside-out pharmacology” [13] (Fig. 1) do assume that drugs cross into the intracellular solution (cytosol)—and, further, into organelles—where they may interact with targets [10, 11, 13, 14]. The principles are general enough to apply to both neurons and glia. We emphasize the chemistry and biophysics of the drug movements. Other contributors to this volume summarize the molecular identity of the targets (when known).

Neurosteroids (also termed neuroactive steroids) partially exert their antidepressant effect by classical effect by binding to GABA<sub>A</sub> receptors. A possible additional role for intracellular neurosteroid targets is less certain than for the examples given above [15].

#### RELATIONSHIP BETWEEN PROTONATION-DEPROTONATION EVENTS AND MEMBRANE PERMEATION OF ANTIDEPRESSANT DRUGS: LOGP, PK<sub>A</sub>, AND LOGD

The hydrophilic chains of the lipid bilayer in the PM and in organellar membranes can more easily accommodate uncharged than charged molecules. Therefore, uncharged molecules diffuse across these membranes more easily than their charged counterparts (given roughly equivalent steric interactions) [16].

Table 1 gathers three important properties that markedly affect a drug’s ability to cross membranes—and therefore, to interact

**Table 1.** Structure and properties of 49 approved and candidate antidepressants.

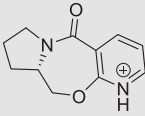
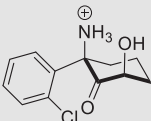
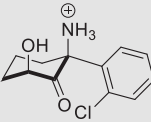
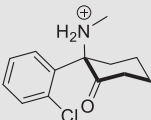
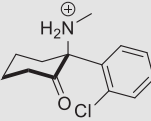
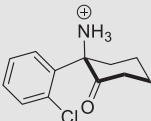
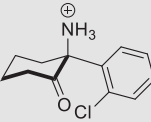
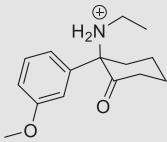
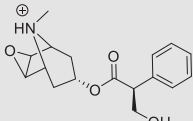
Class	Drug	Protonated Structure	PubChem accession number(s)	LogP	pKa	LogD (pH 7.4)	V <sub>d</sub>
AMPA PAM	Org-26576		13584912	0.78	1.67	0.78	unknown
Ketamine and metabolites	(2R,6R)-hydroxynorketamine		121513910, 137795569	2.04	6.64	1.97	7.3 L/kg (rat)
	(2S,6S)-hydroxynorketamine		71519584, 124201855	2.04	6.64	1.97	7.3 L/kg (rat)
	R-ketamine		644025, 9838417	3.35	7.29	3.10	3–5 L/kg
	S-ketamine		182137, 49852367	3.35	7.29	3.10	3–5 L/kg
	R-norketamine		10105008, 71743680	2.92	7.02	2.76	2–4.25
	S-norketamine		11775775, 71743704	2.92	7.02	2.76	2–4.25
Ketamine analog	methoxetamine		52911279, 71628809	2.94	7.58	2.54	unknown
mAChR antagonist	scopolamine		5184, 638340, 2723877, 3000322, 6451257, 11968014	0.90	6.45	0.85	1.4 L/kg

Table 1. continued

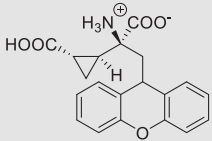
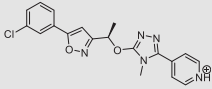
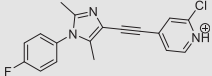
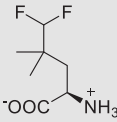
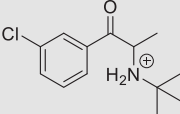
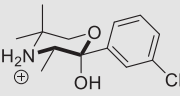
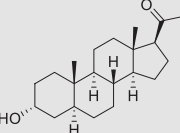
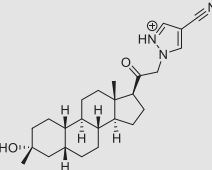
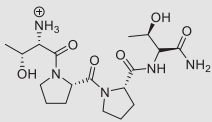
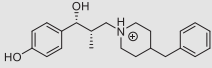
Class	Drug	Protonated Structure	PubChem accession number(s)	LogP	pKa	LogD (pH 7.4)	V <sub>d</sub>
mGluR2/3 antagonist	LY-341495		9819927, 10713043, 57824323	0.22	9.86	−2.93	unknown
mGluR NAM	AZD2066		16041426, 69004954, 69007598	3.36	3.89	3.36	unknown
mGlu <sub>5</sub> R	basimglurant		11438771, 131635700	4.32	5.11	4.31	231 L
mTORC1 activator	NV-5138		129050791	−1.41	9.50	−1.41	unknown
NDRI	bupropion		444, 62884, 11984562	3.27	8.22	2.39	20–47 L/kg
	radafaxine		9795056, 9838996	2.90	7.36	2.62	unknown
Neurosteroid	allopregnanalone		92786, 262961, 6708605	3.99	−1.36	3.99	~3 L/kg
	zuranolone		86294073	3.93	1.36	3.93	>500 L
NMDA co-agonist	rapastinel		14539800, 71311638	−3.71	7.61	−4.13	unknown
NMDA GluN2B antagonist	Ro 25-6981		53250677	3.41	10.03	1.99	unknown

Table 1. continued

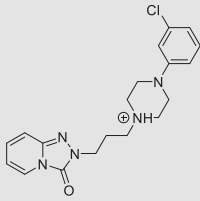
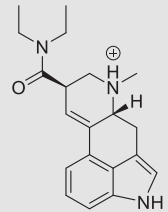
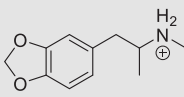
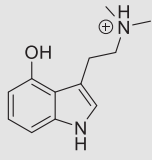
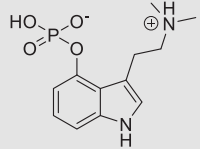
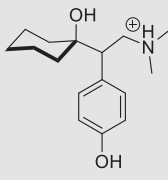
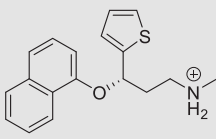
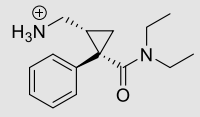
Class	Drug	Protonated Structure	PubChem accession number(s)	LogP	pKa	LogD (pH 7.4)	V <sub>d</sub>
SARI	trazodone		5533, 62935	3.13	8.55	1.96	0.47–0.84 L/kg
Psychedelic	LSD		5761, 159828	2.28	7.03	2.13	32–76 L
	MDMA		1615, 71285	1.86	10.14	−0.76	5.5 L/kg
	psilocin		4980	1.13	9.79	−0.12	2.5–5 L/kg
	psilocybin		10624	−0.14	9.51	−0.89	unknown
SNRI	desvenlafaxine		125017, 25268065	2.19	8.90	0.98	3.4 L/kg
	(S)-duloxetine		60834, 60835	4.20	9.30	2.31	1640 L
	levomilnacipran		6917778, 6917778, 13208116	1.42	9.83	−0.91	387–473 L

Table 1. continued

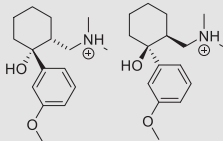
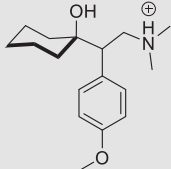
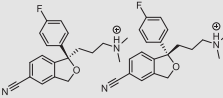
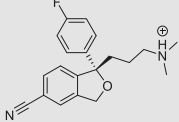
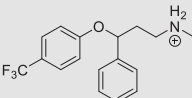
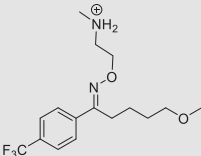
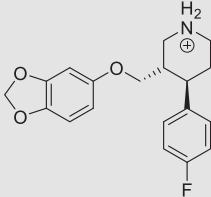
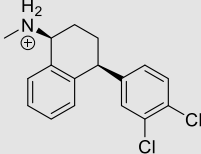
Class	Drug	Protonated Structure	PubChem accession number(s)	LogP	pKa	LogD (pH 7.4)	V <sub>d</sub>
	tramadol		33741, 63013, 44158528	2.45	9.38	0.48	2.6–2.9 L/kg
	venlafaxine		5656, 62923	2.74	9.01	1.12	6–7 L/kg
SSRI	citalopram		2771, 77995,3020376	3.76	10.38	0.89	12 L/kg
	escitalopram, (S)-citalopram		146570, 146571, 9844182	3.76	10.38	0.89	12–26
	fluoxetine		3386, 62857, 13013909	4.17	9.40	2.19	20–42
	fluvoxamine		5324346, 9560989	2.80	8.76	1.42	25 L/kg
	paroxetine		43815, 62878, 6435921, 9845306	3.15	9.32	1.25	3.1–28
	sertraline		63009, 68617	5.15	9.56	3.02	20 L/kg

Table 1. continued

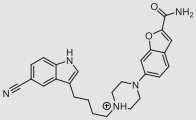
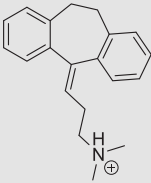
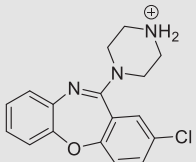
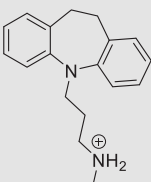
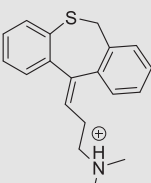
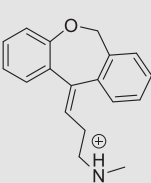
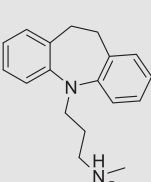
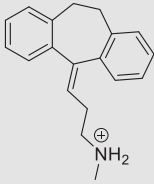
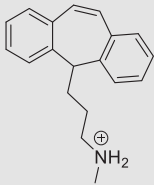
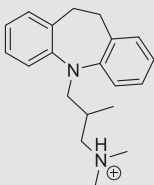
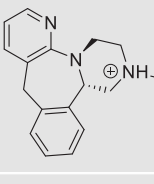
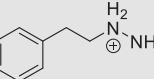
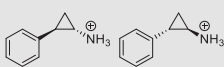
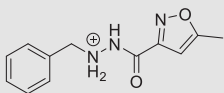
Class	Drug	Protonated Structure	PubChem accession number(s)	LogP	pKa	LogD (pH 7.4)	V <sub>d</sub>
	vilazodone		6918313, 6918314	3.72	9.08	2.03	"Unknown but large"
TCA	amitriptyline		2160, 11065	4.81	9.06	3.15	16 L/kg
	amoxapine		2170, 53339189	3.08	8.83	1.64	"Widely distributed in body tissues"
	desipramine		2995	3.90	10.02	1.37	10–50 L/kg
	dosulepin		5284550, 6420022	4.52	9.06	2.86	45 L/kg
	doxepin		3158, 14675, 667477, 6419921	3.84	9.06	2.18	20 L/kg
	imipramine		3696	4.28	9.20	2.48	10–20 L/kg

Table 1. continued

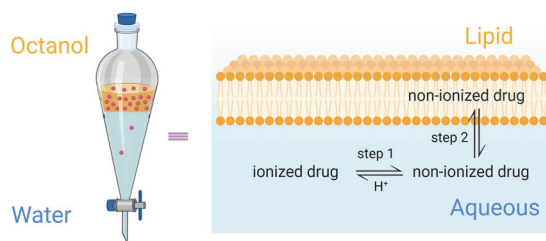
Class	Drug	Protonated Structure	PubChem accession number(s)	LogP	pKa	LogD (pH 7.4)	V <sub>d</sub>
	nortriptyline		4543, 441358	4.43	10.47	1.58	21 L/kg
	protriptyline		4976, 6603149	4.50	11.14	1.37	15–31.2 L/kg
	trimipramine		5584, 107128, 3045275, 5282318	4.76	9.42	2.75	30.9 L/kg
TeCA	mirtazapine		4205	3.21	6.99	3.06	107 L
MAO Inhibitor	phenelzine		3675 61100 28134	1.20	8.18	0.36	"unknown but large"
	tranylcypromine		19493, 25267092, 2723716, 11473982	1.34	8.9	−0.16	1.1–5.7 L/kg
	isocarboxazid		3759	1.43	10.42	1.43	unknown

AMPA AMPA receptor, *mTORC1* mammalian target of rapamycin 1, *NAM* negative allosteric modulator, *NDRI* norepinephrine and dopamine reuptake inhibitor, *PAM* positive allosteric modulator, *SARI* serotonin antagonist and reuptake inhibitor, *TCA* tricyclic antidepressant, *TeCA* tetracyclic antidepressant.

The protonated form is usually given (except for allopregnanolone and zuranolone), because this is typically the form assumed to bind the therapeutic target. PubChem rarely provides the structure of the protonated form. PubChem accession numbers are given for related forms: various salts, neutral forms, and differing trademarks. The PubChem entries also give simplified molecular-input line-entry system (SMILES) and International Chemical Identifier (InChI) ASCII strings for describing the structure of molecules. SMILES and InChI strings can be imported and exported by most molecule editors/viewers to generate 2- or 3-dimensional drawings. Files for Chemdraw, one such editor (.cdx), containing all the structures presented are in Supplement 1.

LogP (usually for the deprotonated form), pKa, and LogD<sub>pH7.4</sub> were calculated in April through August, 2023 by Chemicalize, <https://chemicalize.com/>, developed by Chemaxon. V<sub>d</sub> is taken from DrugBank where available, otherwise from various literature sources. V<sub>d</sub> values are from human experiments, except where stated. V<sub>d</sub> is measured either as L/kg of body mass or simply as L (human body is ~70 kg).





• LogP is measured for step 2 only, partitioning of a drug's neutral, non-ionized form.

• LogD =  $\log_{10}$  of the distribution coefficient (D) for the sum of all the drug's forms (ionized + non-ionized)

• LogD<sub>pH7.4</sub> =  $\log_{10}$  of the distribution coefficient (D) at physiological extracellular pH.

For a base with a single protonated group, we calculate for LogD<sub>pH7.4</sub> by including step 1:

$$\text{LogD}_{\text{pH7.4}} = \text{LogP} - \log [1 + 10^{(7.4 - \text{pK}_a)}]$$

**Fig. 2** The concept of LogP and LogD<sub>pH</sub>. For example, a drug with LogP = 1 and pK<sub>a</sub> of 7.4 would have LogD<sub>pH7.4</sub> = 1 – log(1 + 100) = 1 – log(2) = 0.7. Created with BioRender.com.

with target sites that face the cytoplasm or the lumen of organelles. LogP, a classic metric (also called the octanol-water partition coefficient), is measured at room temperature. Early on, octanol or olive oil were considered possible models for cell membranes. The experiments were performed by adding octanol, water, and the test compound to a separatory funnel (Fig. 2). After shaking, the experimenter eluted the two phases separately, then measured the amount of the test compound in each phase. LogP is the logarithm (base 10) of the octanol:water concentrations. Many additional experimental techniques are now available to supplant the separatory funnel of Fig. 2, but octanol remains useful for representing some aspects of membranes [17, 18]. LogP is now often predicted by one or more algorithms based on the compound's formula, substructures, topology, or other properties [19]. These predictions typically vary by 0.5 to 1 log unit for a single molecule. The LogP data in Table 1 derive from extensions of a classical algorithm [20, 21]. Some compilations use a "consensus logP" (cLogP) which averages predictions of several algorithms.

As a rough approximation, lipophilic compounds (LogP > ~0) more easily enter the membrane bilayer. Thus, LogP can determine the availability of potential neuropsychiatric compounds in the brain, as crossing the blood-brain barrier (BBB) is necessary for any CNS-active molecule to exert its effects.

However, a limitation of LogP is that only non-ionized molecules are included in the solubility measurements; because of pH-dependent protonation-deprotonation reactions, a significant percentage of molecules remains excluded from the measurement or calculation. Therefore, Table 1 also presents the acid dissociation constant, pK<sub>a</sub>. This metric instantiates the tendency of a chemical species to gain or lose hydrogen ions (protons, H<sup>+</sup>) in aqueous solution at a specific pH. At a pH equal to the pK<sub>a</sub>, the drug molecules are 50% charged, and 50% are uncharged. For each increment in pH, this balance changes by roughly 10-fold (Fig. 2).

Most psychiatric drugs are weakly basic because they contain an amine moiety that can exist in both protonated (charge +1) and deprotonated (neutral) forms. An important implication of this concerns physiological blood and CSF pH (7.4 and 7.3, respectively [22]; we use 7.4 in this review, as in most compendia). If the drug's pK<sub>a</sub> is higher than the local pH, most molecules exist in their protonated form; and if lower, then most exist in their deprotonated form.

Some candidate psychiatric drugs are weak acids. In this case, the neutral form exists at pH < pK<sub>a</sub>; and at pH > pK<sub>a</sub>, the deprotonated negative form (charge = –1) predominates. In all known cases, protonation-deprotonation reactions of small

molecules take place in milliseconds. On the usual pharmacological time scale, this reaction is not expected to distort the dynamics of any processes considered here.

For these and other reasons, LogD<sub>pH<sub>X</sub></sub>, the distribution coefficient at pH X, is necessary for understanding the actions of brain-permeant weak bases (Fig. 2, Table 1). LogD incorporates the fractional ratio of the much more permeant, uncharged compound in water. As noted, for CNS-active drugs, one typically uses the pH of the blood; thus, we usually discuss LogD<sub>pH7.4</sub>. For the case of a compound with only a single protonation-deprotonation group, a straightforward equation calculates LogD from LogP and pK<sub>a</sub> (Fig. 2) (Note that pK<sub>a</sub> is, itself, often determined algorithmically).

In fact, pH varies throughout the body, with both intracellular compartments (see next section) as well as parts of the digestive tract retaining a lower pH setpoint, thereby influencing both ionization and lipophilicity particularly for ingested compounds.

Because many factors influence the distribution of drugs in target organs, cells, organelles, and membranes (see below), LogD is most useful as a comparison among drugs with similar chemistry and/or mode of action. For example, among compounds that serve as nicotinic agonists, compounds with LogD<sub>pH7.4</sub> values as low as –1, such as varenicline, may enter the CNS at sufficient rates to be useful when given orally [23, 24]. Entry is only part of the evaluation; the rate of metabolism is also crucial, as described below (Pharmacokinetic aspects of ketamine, its metabolites, and analogs).

We point out that no LogP or LogD algorithms are stereoselective. S-ketamine (esketamine) and R-ketamine (arketamine) show no differences in these two metrics; neither do citalopram and S-citalopram (escitalopram) (Table 1).

## SUPRACELLULAR PHARMACOKINETICS IS TYPIFIED BY LIPINSKI'S GENERALIZATIONS

Medicinal chemistry campaigns for orally active drugs must usually pass a threshold that summarizes a set of observations assembled by Lipinski and colleagues during the 1990s [25], based on aggregated features of Phase II trial compounds. The criteria for good oral bioavailability are: molecular weight (MW) < 500 g/mol; LogP < 5; < 5 hydrogen (H)-bond donors, calculated by counting amine (–NH<sub>x</sub>, where x = 0–3) and hydroxyl (–OH) groups; and < 10 H-bond acceptors, calculated by adding nitrogen atoms and oxygen atoms. Failure to satisfy two or more rules drastically increases the chances of poor oral absorption, and compounds which act as substrates for biological transporters (e.g. antibiotics, antifungals, vitamins, cardiac glycosides) comprise the vast majorities of the exceptions to these rules [25]. A successful update to the criteria included replacement of LogP by LogD<sub>pH7.4</sub> [26]. Nonetheless, once a compound has satisfied the Lipinski criteria, they provide no further information whether/why/how a drug may work, or whether it may be cytotoxic.

Metabolic transformation of drugs, mostly in the liver, is an important component of supracellular pharmacokinetics [27]. We briefly treat metabolic transformations of individual RAAD molecules below (Other aspects of ketamine and its metabolites).

## VOLUME OF DISTRIBUTION HAS BOTH SUPRACELLULAR AND SUBCELLULAR COMPONENTS

V<sub>d</sub> describes the propensity of a drug to accumulate in compartments aside from free, unbound drug in the plasma [28]. The units of measurement of V<sub>d</sub> are volume divided by the total mass of the animal. The usual units are liters/kg (where the volume represents the volume of protein-free, lipid-free solution that would be necessary to hold the compound at the same concentration as in the plasma). A useful way to present this relationship is  $V_d = V_p + V_t \left( \frac{f_{up}}{f_{ut}} \right)$ , where V<sub>p</sub> is plasma volume, V<sub>t</sub> is

tissue volume,  $fu_p$  is fraction unbound in plasma, and  $fu_t$  is fraction unbound in tissue. We appreciate this equation because it emphasizes the unbound drug molecules; these are available in aqueous solution to channels, receptors, transporters, or other targets. At the low concentrations typical of neuropharmaceuticals, this concentration equals the chemical activity of the drug. Drugs with lower  $V_d$  also tend to remain in the plasma, while drugs with higher  $V_d$  tend to become bound in other tissues. If a drug is present and unbound only in the total body water,  $V_d$  depends on age, sex, height, and weight. For healthy adults,  $V_d$  averages 0.75 l/kg (total body water averages 750 ml/kg) [29]; but this includes the rather low volume of distribution in bone and adipose tissue. In brain,  $V_d \sim 0.78$  l/kg [30].

Until recently,  $V_d$  was measured indirectly in animals and humans [27], by the clearance of a drug (or its metabolites) into excreted biofluids. In some cases, metabolism of the drug and subsequent elimination is saturated, so that the dynamics of disappearance becomes linear rather than exponential, sometimes requiring several days.

Measurements of  $V_d$  fall in surprisingly high ranges (see Table 1). At the low end,  $Cl$  has a  $V_d$  of  $\sim 0.4$  l/kg—roughly equal to the extracellular volume in an organism. At the high end is chloroquine,  $\sim 200$  l/kg [31]. Among antidepressants, tricyclics (TCAs) and SSRIs have relatively high  $V_d$  (20–40 l/kg); SNRIs and S-ketamine have much lower values, comparable to nicotine ( $\sim 2.8$  l/kg). Higher  $V_d$  is usually associated with (a) slower initial buildup of a drug to effective doses and (b) slower elimination from the body. Although (b) is rather obvious, (a) is less evident. Buildup is slower because the drug must be allowed to accumulate via small, infrequent doses that avoid overshooting the therapeutic range. Spreadsheets and commercial software are available to achieve this result.

Where “is” most of a drug that has a high volume of distribution? Three compartments are possible. The first is reversible binding to proteins. A common drug-binding protein is serum albumin, and this binding, like many drug-protein binding events, is often stereoselective [32, 33]. We know of no general studies on the possible stereoselectivity of psychiatric drugs to albumin. The second and third components are primarily subcellular, as described in the next sections.

## SUBCELLULAR PHARMACOKINETICS

Although some aspects of accumulation in organelles appeared in the Nobel Prize-winning work of Mitchell [34] and de Duve [35], broadly applied measurements of subcellular pharmacokinetics are relatively new, depending on advances that have been applied since  $\sim 2010$ . Two of the most appropriate methods are highly parallel mass spectrometry [36–40] and genetically encoded, intensity-based drug-sensing fluorescent reporters [14, 24, 41–43]. These experiments showed, for example, that the cellular accumulation of both escitalopram and fluoxetine as measured *in vitro* are among the largest recorded for any drug [39, 43].

An important component of subcellular  $V_d$  is binding to membranes. The propensity of a drug to bind to membranes is not fully captured by  $\text{LogD}_{\text{pH}7.4}$ , because weak bases with modestly high  $\text{LogD}_{\text{pH}7.4}$  ( $> \sim 3$ ) tend to have higher  $V_d$  due to interactions between positively charged nitrogen atoms and negatively charged phospholipid head groups [28, 44]. In contrast to drug-protein interactions, drug-lipid binding is not stereoselective.

Indeed, when antidepressant partitioning into lipids was measured directly using isothermal titration calorimetry (ITC), partitioning showed a poor correlation with  $\text{LogP}$  or  $\text{LogD}_{\text{pH}7.4}$  [44]. The ITC measurements did correlate well with the antidepressants' action on the gramicidin A monomer-dimer equilibrium in lipid bilayers, a sensitive and historically important monitor of membrane protein conformational changes. After comparing their gramicidin A channel data with previous data on

the function of membrane proteins (ion channels, receptors, and transporters) in the presence of antidepressants, Kapoor et al. [44] concluded that “both gramicidin A channels and [other] integral membrane proteins respond to similar changes in lipid bilayer properties.” Individual antidepressants may vary in their effects on lipid bilayer properties such as curvature [45], thickness [46], and fluidity [47].

In addition to the antidepressant effects on these properties of spatially uniform lipid bilayer models, local membrane fluidity is influenced by the presence of lipid rafts, which are cholesterol-, sphingomyelin-, and cytoskeleton-rich regions that stiffen the membrane and regulate cellular signaling [48]. Lipid rafts can also store  $G_{s\alpha}$  (the subunit of  $G_s$  that stimulates adenylyl cyclase signaling [49]), where it has reduced ability to elevate cAMP [50, 51]. Interestingly,  $G_{s\alpha}$  can be translocated to non-raft membrane sections after the chronic (multi-day) administration of various types of antidepressants, such as TCAs [52, 53], SSRIs [52–54], SNRIs [53], and atypical antidepressants [53]. In recent data, the interaction of ketamine with raft domains during a brief (15 min) incubation exerted the same effects on  $G_{s\alpha}$  translocation [48], indicating that this may present a common mechanism for increasing intracellular signaling in patients with major depressive disorder (MDD) who have dysregulated cAMP signaling [50]. The degree to which ketamine and other RAADs differ from typical antidepressants in their  $G_{s\alpha}$ -displacing effects is as yet not well understood (though (2 R,6 R)-hydroxynorketamine, (2 R,6 R)-HNK) likewise displaces  $G_{s\alpha}$  from raft domains after transient exposure [48], indicating a potential temporal commonality among RAADs but may depend on their ability to access lipid raft domains only briefly. From this viewpoint, the accumulation of typical antidepressants in rafts [55] may be sufficient but not necessary to upregulate aberrant cAMP signaling and reflect the tendency of non-RAADs to stay in the membrane phase, thereby slowing their therapeutic effects [56].

A recent report increases the evidence that antidepressants can perturb lipid rafts [57]. Ketamine, (2 R,6 R)-HNK, fluoxetine, and imipramine all bind directly to the transmembrane helices of the BDNF receptor TrkB, potentially even at the same site [57]. All these antidepressants facilitated upregulation of TrkB signaling in a cholesterol-dependent manner at clinically relevant concentrations [57]. Thus, antidepressants change TrkB interactions with membrane cholesterol. Molecular dynamic simulations show that the uncharged, neutral form of ketamine is likely to be binding to TrkB [57]. Because the uncharged form is accumulated by several orders of magnitude within the membrane phase, the membrane phase is likely to provide the ketamine molecules for this interaction.

In general, however it is not known whether drugs that accumulate within the PM can reach their targets via entry preferentially from the membrane phase, compared with entry from the aqueous phase [58]. For multidrug transporters, the membrane approach seems unlikely [59]. Use of impermeant quaternary analogs of drugs is a venerable paradigm in ion channel and receptor pharmacology [14, 58, 60]. A recent paper reported analogous experiments with SERT [56]. The data revealed only modest decreases in affinity for the impermeant derivatives (6- to 10-fold), providing little support for the membrane approach mechanism. The live-cell experiments with fluorescent biosensors were limited by the viability of the cells (2.4 h). Nonetheless, the impermeant derivatives will provide a convenient probe to distinguish effects of SERT blockade from effects of intracellular SSRI-SERT interactions. Similarly, recent experiments with impermeant quaternary analogs of psychedelic drugs distinguished intracellular from PM effects [6].

The largest myelinated axons have hundreds of lipid-rich myelin layers, all capable of serving as sinks for drugs with high  $\text{LogD}$ . We recently discussed the hypothesis that diffusion and accumulation within myelin can explain the “therapeutic” lag of 2–6 weeks for SSRIs. In sum, the hypothesis is unlikely but not inconceivable [56].

### "ACID TRAPPING" AND POTENTIAL-DEPENDENT ACCUMULATION IN SUBCELLULAR PHARMACOKINETICS

Another component of subcellular  $V_d$  is "acid trapping" of weak bases in acidic organelles such as lysosomes, endosomes, and synaptic vesicles. Once acidic organelles take up the neutral form of a weakly basic drug, a predictable fraction of those molecules become protonated and therefore unable to cross back into the cytosol. This mechanism was predicted by de Duve soon after he first isolated lysosomes, including his references to earlier literature on the existence of acidic compartments within cells [35]. The theoretical maximal accumulation of a weakly basic drug with a single protonation site, versus blood, increases by 10-fold for every unit of difference between the pH of the organellar lumen and that of the blood (Fig. 3). An adequate theory of acid trapping must account for the efficiency of the pumps that maintain organellar pH, the pKa of the compound, the (small) membrane permeability of the charged species, the charge on the protonated drug, the membrane potential of the organelle, and other factors [35, 56, 61]. Several quantitative models converge on the idea that drugs with pKa ~8 may accumulate most markedly in lysosomes [35, 56, 61].

Among mammalian cells, one expects drugs in lysosomes (which account for 0.5%–3% of the cellular volume) to increase the total cellular content of a singly charged, weakly basic drug by several fold [35]. The predicted accumulation factor is much larger for doubly charged drugs [62]. The best-understood therapeutic role for acid trapping of a drug, though not relevant to psychiatry, may be chloroquine in lysosomes, and this action likely includes events downstream from modest induction of lysosomal stress [63]. Some drugs accumulate so strongly that they precipitate in lysosomes [64]. Sometimes such precipitates vitiate therapeutic

use of the drug [65]; but these negative results in drug discovery campaigns are rarely reported in the literature. Acid trapping is not thought to be stereoselective.

In neuroscience, attention has also focused on drug accumulation in synaptic vesicles in axon terminals [66, 67]. The luminal pH of synaptic vesicles is ~5.5, ~1 unit higher than lysosomes (Fig. 3); therefore, accumulation in synaptic vesicles would probably avoid the drastic effects (good and bad) of lysosomal accumulation. Substantial accumulation in synaptic vesicles has, in fact, been demonstrated for antipsychotic drugs [61, 68]. Action potentials can release the accumulated antipsychotic drugs from these vesicles [61].

Note that the predicted ratio in Fig. 3 is less than unity for the mitochondrial matrix, which is more basic than the cytosol or the blood. However, accumulation in mitochondria may be greatly modified by the membrane potential of the organelle, an effect not considered by de Duve [35] but measured semiquantitatively [69] and analyzed theoretically [70] in later investigations. If the plasma membrane and the organelle membrane are permeable to the cationic form of the drug, the cation would be distributed, at equilibrium in the organellar lumen, according to the Nernst potential for the algebraically summed resting potentials of the plasma membrane and the organellar membrane. For mitochondria, the luminal (matrix) resting potential vs cytoplasm (~−180 mV) would add to the resting potential of the neuronal cytoplasm vs CSF/blood (−70 to −90 mV). The suggestion that SSRIs accumulate in mitochondria has never been measured directly but should be considered in view of the several reports that SSRIs, especially fluoxetine, decrease respiratory functions of mitochondria [71, 72].

Direct measurements of drug levels in acidic organelles in live cells face the challenge that GFP fluorescence decreases at pH~6.5

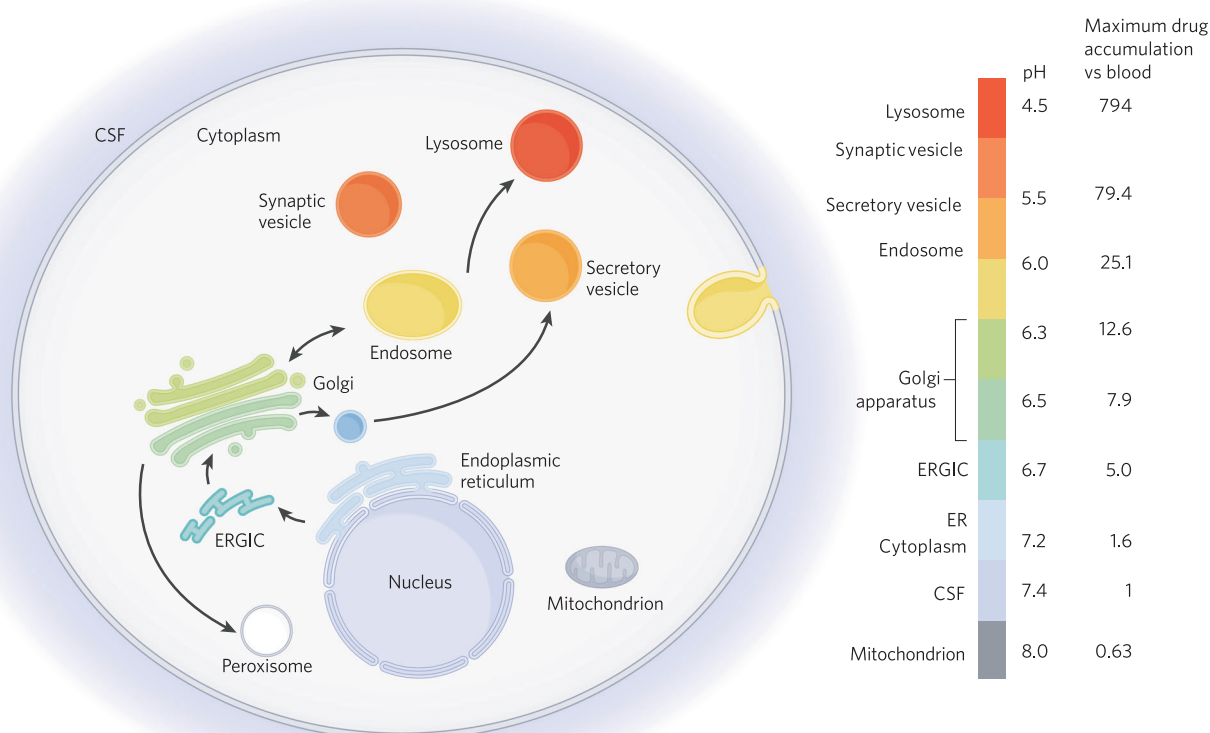


**Fig. 3 Weak bases accumulate in acidic vesicles.** The major classes of organelle are arranged on a vertical scale denoting their approximate luminal pH. At right, we show the maximum possible equilibrium accumulation for a monovalent weak base, versus blood (pH 7.4), as predicted by de Duve [35]. The vesicles are not drawn to relative scale; and only a few of the major trafficking pathways are shown. The pH of the peroxisomal lumen remains uncertain; therefore, no color is applied. ERGIC endoplasmic reticulum-Golgi intermediate compartment.



and below [73]. Therefore, GFP-based fluorescent sensors for antidepressants like those our lab has developed (iDrugSnFRs [41, 56]) become insensitive in the lumen of acidic organelles. Other fluorescent proteins, such as mTurquoise, do function at lower pH [74]; and in our preliminary data, mutating the GFP moiety allows iDrugSnFRs to function at pH as low as pH 4.5. In fluorescent sensors based on G protein-coupled receptors [75, 76], the fluorophore faces the cytosol rather than the lumen; and these sensors may become useful for quantitative studies of drugs in acidic organelles.

### SPINE SYNAPSES

Neuroplasticity at the level of spine synapses is often invoked to explain the action of antidepressants which are thought to remodel existing spines or create new ones [77–82]. To our knowledge, no data exist on whether antidepressants accumulate preferentially within the presynaptic terminal, postsynaptic cytoplasm, or postsynaptic density (see next paragraph) of spine synapses. Within the limits of the optical resolution provided by a spinning-disk confocal microscope, fluorescent biosensors for SSRIs provided no evidence that SSRIs accumulate within the presynaptic terminal or postsynaptic cytoplasm [56].

### MEMBRANE-LESS ORGANELLES

Membrane-less organelle-like structures of interest to neuroscience include presynaptic release zones [83], the postsynaptic density of glutamatergic synapses [84], the subsynaptic zone of the nerve-muscle synapse [85], and some protein-RNA foci in neurodegenerative diseases [86, 87]. These may result from protein and/or RNA phase separation, in which a well-mixed solution containing macromolecules separates into a dense phase and a dilute phase. The dense phase can in certain instances function as an intracellular compartment. Water states and hydration differ in dense macromolecular phases from their characteristics in cytosol [88], almost certainly leading to altered values of LogP and pKa for any drug. We expect profound consequences for local pharmacology and pharmacokinetics in the dense phases of membrane-less organelles; but we are unaware of any literature on this topic.

### PHARMACOKINETIC ASPECTS OF KETAMINE, ITS METABOLITES, AND ANALOGS

The physical and chemical principles described above operate within the constraints of enzymatic metabolism, both before and after the drug reaches the brain. Therefore, this section concentrates on metabolism of candidate and approved RAADs, with additional comments on newly discovered mechanistic points. Nearly all drug metabolizing enzymes are intracellular, mostly in the ER. This reminds us, again, that the effects of antidepressants depend on their entry into cells and organelles.

Ketamine meets all Lipinski criteria, but it has poor bioavailability in clinical studies (24%) [89] due to efficient metabolism by liver enzymes [90–96] which act, in part, before the drug crosses substantially into the brain. Ketamine has a chiral center, with (S) and (R) enantiomers (Table 1). The two enantiomers differ in their interaction with NMDAR receptors, perhaps explaining differences in the clinical effects [97–103]. Here, we emphasize that ketamine metabolism is also stereospecific [104], and all metabolites likewise retain chiral centers. The enantiomers do not interconvert [105]. All these features allow for the independent study of each enantiomer and its effects on human physiology.

Compared with plasma concentrations among patients receiving IV ketamine for anesthesia and analgesia, antidepressant doses result in plasma concentrations an order of magnitude lower than the former but similar to the latter (0.32–0.78  $\mu$ M) [96, 106, 107].

Across its various clinical applications, ketamine infusion is the most common mode of administration because of the rapidity with which plasma levels reach desired concentrations, but this route of administration may present challenges to clinics with fewer resources. Intramuscular (IM) injections have high bioavailability in adults [108] but present similar structural barriers as the IV route, and oral administration achieves a bioavailability of only 24% [89] due to the aforementioned efficient liver metabolism [96]. In contrast, intranasal (IN) administration has proved both efficacious and easier to implement with patients. IN bioavailability is higher than that found for oral administration (45%) [93], likely due in part to a more rapid entry into plasma as well as bypassing first-pass metabolism by the liver [96]. Placebo-controlled studies administering antidepressant doses of ketamine to patients with MDD demonstrated significant relief of depression symptoms within a day [109–114], and, overall, there appears to be little difference in short-term antidepressant efficacy between the IV and IN routes [115]. Indeed, this latter regimen is the basis for the 2019 approval by the FDA of the intranasal esketamine formulation Spravato® for treatment-resistant depression.

Ketamine and esketamine were recently shown to bind to the BDNF receptor TrkB, which was shown to mediate many of the plasticity-promoting effects *in vitro* and in mice [7, 57], but whether arketamine also binds to TrkB remains to be investigated. Several clinical trials are underway to assess arketamine as an antidepressant in IV formulations [116, 117], with one trial showing significant reduction in clinician-assessed depression scores one day post-infusion without a concomitant increase in clinical dissociation scores [116].

However, ketamine's metabolites are metabolized and eliminated on longer time scales [95]. Therefore, some RAAD research has focused on several primary and secondary metabolites of ketamine. Interest in the potential antidepressant effects of ketamine metabolites was previously generated from studies which raised questions about the relationship between ketamine metabolism and therapeutic relief [95, 106], and there was even an indication that the metabolism of ketamine was correlated with both better response as well as side effects [106]. Along the major metabolic pathways, racemic ketamine, R-ketamine, or S-ketamine is metabolized stereospecifically into the corresponding HNK enantiomer. Stereospecific transformations also produce various (R,S)-dehydroxynorketamine (DHNK) metabolites [96, 118]. All HNK molecules retain the original chiral site while also adding another in the cyclohexanone ring [96]. Minor pathways produce 4- and 6-hydroxyketamine as well as (2 R,6 R; 2 S,6 S)-HNK primary metabolites [96]. These metabolites can appear as early as 40 min after the end of IV infusion [95, 106] and reach peak plasma levels within four hours [95], with the eventual ratio of (S)-metabolites to (R)-metabolites always less than one [95, 119]. In rodents, both parent compounds and metabolites accumulate in the brain within ten minutes post-infusion [120–123], with at least one study reporting higher concentrations of (S)-metabolites than (R)-metabolites in the brain [121], though with no appreciable difference in the brain-to-plasma ratio of either set of enantiomers indicative of enantioselective uptake [96]; additionally, all metabolites cross the BBB less effectively than the parent compound [124]. (2 R,6 R; 2 S,6 S)-HNK also appears to meet all Lipinski criteria and does appear to have higher oral bioavailability than its parent compound (46–52% in mice and 42–46% in rats) [104, 123]. In humans, while ketamine in plasma drops below detection within one day of an IV antidepressant dose (0.5 mg/kg over 40 min), DHNK and (2 R,6 R; 2 S,6 S)-HNK can be detected up to three days post-infusion in patients [95, 119].

An influential study investigated the antidepressant activity of ketamine metabolites in rodent models of depression [124]. In all, results suggest that several primary and secondary ketamine metabolites potentially offer RAAD treatment of MDD symptoms

but with a much lower side effect profile. (2R,6R)-HNK was found to produce antidepressant-like effects in rodents, but it did not bind to NMDA receptors at concentrations that produce antidepressant-like effects [124]. 2R,6R-HNK was subsequently found to bind to TrkB, and its plasticity-promoting effects are lost in TrkB mutants with poorer affinity [14, 58, 60]. However, a recent study failed to find any binding sites for (2R,6R)-HNK [125] although the binding to TrkB was investigated at lower concentrations than that previously found to be needed for TrkB binding [57].

### OTHER RAAD CANDIDATES

A class of drugs with functional groups resembling ketamine has garnered attention over the past decade based first on anecdotal reports that these compounds relieve the symptoms of depression [126–129].

The first drug from this class to offer intriguing results, methoxetamine (MXE), was synthesized for recreational use in 2010 to mimic the dissociative effects of ketamine at lower concentrations while mitigating against ketamine's urotoxicity [130]. MXE meets all Lipinski criteria; as no data are available concerning its oral bioavailability in humans, we might assume it would be somewhat higher than ketamine, owing to far less extensive hepatic metabolism (75% of MXE injected into rodents is extracted unchanged after one day [131]). Like ketamine, MXE is thought to act as a noncompetitive NMDAR antagonist, with slightly higher affinity ( $K_i = 0.259 \mu\text{M}$ ) than ketamine ( $K_i = 0.659 \mu\text{M}$ ) for the PCP site [132]; it also inhibits SERT at low concentrations ( $K_i = 0.481 \mu\text{M}$  [132] and  $\text{IC}_{50} = 2 \mu\text{M}$  [133]), unlike ketamine and more potently than PCP ( $K_i = 2.234 \mu\text{M}$  [132]), and it can also inhibit the NE transporter (NET;  $\text{IC}_{50} = 20 \mu\text{M}$ ) and the DA transporter (DAT;  $\text{IC}_{50} = 33 \mu\text{M}$ ) [133], unlike ketamine [132]. In a rodent study, MXE fully generalized to ketamine in an operant conditioning task assessing psychomimesis in a dose-dependent manner, indicating similar subjective effects [134], and it also demonstrates the typical dose-dependent ketamine profile of inducing angiogenic effects at lower doses while acting as a dissociative anesthetic at higher doses [131, 135]. MXE's effects endure for longer than those of ketamine in rodents [131, 136], consistent with case reports and testimony from users [126, 127], reaching peak concentration in rat brain slower than ketamine (30 min [131] versus within 10 min [120–123]) but at a higher maximal concentration than ketamine (1–7  $\mu\text{M}$  [131] versus ~9  $\mu\text{M}$  [136]) and becoming undetectable after six hours [131] as opposed to within two hours with ketamine [136].

Scopolamine, while comprising a much different set of functional groups than the aforementioned candidate RAADs, also meets all Lipinski criteria, and is known to cross into the brain more easily than most anticholinergics; however, it has limited oral bioavailability (13%), which could also be due to extensive first-pass hepatic metabolism [137]. In all, these RAADs appear to differ in their oral bioavailability because of their metabolic profiles.

### PRODRUG ASPECTS OF AN ANTIDEPRESSANT AND A PSYCHEDELIC DRUG

The atypical antidepressant bupropion acts in part as a prodrug, via action of cytochrome P450 2B6 to produce (2S,3S)-hydroxybupropion. The latter is at least as active as bupropion itself [138].

Psilocybin is metabolized via alkaline phosphatase to its active psychedelic metabolite, psilocin. LSD and psilocin have recently shown promise as potent, fast-acting, and long-lasting antidepressants [80, 139]; promotion of neuroplasticity has been considered important for their antidepressant actions [140]. The effects of psychedelics are considered to be mediated by their binding to 5HT<sub>2A</sub> receptors, and 5HT<sub>2A</sub> receptor antagonists indeed block the hallucinogenic effects of these compounds

[140, 141]. However, it was recently proposed that the hallucinogenic effects can be separated from the plasticity-promoting effects [82], and binding to intracellular 5HT<sub>2A</sub> receptors has been suggested as the pathway mediating the plasticity-promoting effects [6]. In other recent data, LSD and psilocin bind to TrkB receptors with high affinity, thereby sensitizing TrkB to BDNF, and their plasticity-promoting and antidepressant-like effects are mediated by TrkB; but the hallucinogenic effects are produced through 5HT<sub>2A</sub> receptors [7].

### INTRACELLULAR TARGETS MUST BE CONSIDERED IN ANTIDEPRESSANT ACTION

Our friends ask how the fraction of antidepressants that act intracellularly differs from drugs for other therapeutic areas. We have performed no systematic survey on this point. We do respond, heuristically, that many classes of drugs in non-neuronal areas, such as those for cancer and diabetes, block enzymes which are primarily intracellular. In fact, outside the brain, most low-molecular weight drugs are *assumed* to bind intracellularly. Psychiatry presently has few such targets, although example (1) in the Introduction—MAO inhibitors—provide a longstanding counterexample. As intracellular targets become more established—see example (5) in the Introduction—we may witness introductions of additional neuropsychiatric medications that engage with intracellular targets. In the areas generally described as “neuropsychiatric”, neurology may eventually represent the outlier with a great proportion of PM targets, because of its heavy reliance on manipulating the ion channels, receptors, and transporters that directly govern membrane excitability. Other papers in this volume review the targets, the transduction mechanisms, and the circuit consequences of antidepressants. For the present, this review reminds researchers in neuropsychopharmacology that intracellular molecules could—and often do—also serve as primary targets of engagement.

### REFERENCES

- Levitt P, Pincus JE, Breakefield XO. Immunocytochemical demonstration of monoamine oxidase B in brain astrocytes and serotonergic neurons. *Proc Natl Acad Sci USA*. 1982;79:6385–9.
- Westlund KN, Krakower TJ, Kwan SW, Abell CW. Intracellular distribution of monoamine oxidase A in selected regions of rat and monkey brain and spinal cord. *Brain Res*. 1993;612:221–30.
- Greenawalt JW, Schnaitman C. An appraisal of the use of monoamine oxidase as an enzyme marker for the outer membrane of rat liver mitochondria. *J Cell Biol*. 1970;46:173–9.
- Cade JF. Lithium salts in the treatment of psychotic excitement. *Med J Aust*. 1949;2:349–52.
- Jakobsson E, Argüello-Miranda O, Chiu SW, Fazal Z, Kruczek J, Nunez-Correa S, et al. Towards a unified understanding of lithium action in basic biology and its significance for applied biology. *J Membr Biol*. 2017;250:587–604.
- Vargas MV, Dunlap LE, Dong C, Carter SJ, Tombari RJ, Jami SA, et al. Psychedelics promote neuroplasticity through the activation of intracellular 5-HT<sub>2A</sub> receptors. *Science*. 2023;379:700–06.
- Moliner R, Giry M, Brunello CA, Kovaleva V, Biojone C, Enkavi G, et al. Psychedelics promote plasticity by directly binding to BDNF receptor TrkB. *Nat Neurosci*. 2023;26:1032–41.
- Nardou R, Sawyer E, Song YJ, Wilkinson M, Padovan-Hernandez Y, de Deus JL, et al. Psychedelics reopen the social reward learning critical period. *Nature*. 2023;618:790–8.
- Sun N, Qin YJ, Xu C, Xia T, Du ZW, Zheng LP, et al. Design of fast-onset antidepressant by dissociating SERT from nNOS in the DRN. *Science*. 2022;378:390–98.
- Henderson BJ, Lester HA. Inside-out neuropharmacology of nicotinic drugs. *Neuropharmacology*. 2015;96:178–93.
- Stoeber M, Jullie D, Lobingier BT, Laeremans T, Steyaert J, Schiller PW, et al. A genetically encoded biosensor reveals location bias of opioid drug action. *Neuron*. 2018;98:963–76.e5.
- Williams JT, Ingram SL, Henderson G, Chavkin C, von Zastrow M, Schulz S, et al. Regulation of mu-opioid receptors: desensitization, phosphorylation, internalization, and tolerance. *Pharm Rev*. 2013;65:223–54.

13. Lester HA, Miwa JM, Srinivasan R. Psychiatric drugs bind to classical targets within early exocytotic pathways: therapeutic effects. *Biol Psychiatry*. 2012;72:905–15.
14. Shivange AV, Borden PM, Muthusamy AK, Nichols AL, Bera K, Bao H, et al. Determining the pharmacokinetics of nicotinic drugs in the endoplasmic reticulum using biosensors. *J Gen Physiol*. 2019;151:738–57.
15. Maguire JL, Mennerick S. Neurosteroids: mechanistic considerations and clinical prospects. *Neuropsychopharmacology*. 2023. <https://doi.org/10.1038/s41386-023-01626-z>. Epub ahead of print.
16. McLaughlin S, Eisenberg M. Antibiotics and membrane biology. *Annu Rev Biophys Bioeng*. 1975;4:335–66.
17. Hessa T, Kim H, Bihlmaier K, Lundin C, Boekel J, Andersson H, et al. Recognition of transmembrane helices by the endoplasmic reticulum translocon. *Nature*. 2005;433:377–81.
18. Wimley WC, Creamer TP, White SH. Solvation energies of amino acid side chains and backbone in a family of host–guest pentapeptides. *Biochemistry*. 1996;35:5109–24.
19. Mannhold R, Poda GI, Ostermann C, Tetko IV. Calculation of molecular lipophilicity: state-of-the-art and comparison of LogP methods on more than 96,000 compounds. *J Pharm Sci*. 2009;98:861–93.
20. Viswanadhan VN, Ghose AK, Revankar GR, Robins RK. Atomic physicochemical parameters for three dimensional structure directed quantitative structure-activity relationships. 4. Additional parameters for hydrophobic and dispersive interactions and their application for an automated superposition of certain naturally occurring nucleoside antibiotics. *J Chem Inf Comput Sci*. 1989;29:163–72.
21. Chemaxon. logP Plugin. 2023. <https://docs.chemaxon.com/display/docs/logp-plugin.md#calculation-method>.
22. Bradley RD, Semple SJ. A comparison of certain acidbase characteristics of arterial blood, jugular venous blood and cerebrospinal fluid in man, and the effect on them of some acute and chronic acid-base disturbances. *J Physiol*. 1962;160:381–91.
23. Rollema H, Chambers LK, Coe JW, Glowa J, Hurst RS, Lebel LA, et al. Pharmacological profile of the  $\alpha 4\beta 2$  nicotinic acetylcholine receptor partial agonist varenicline, an effective smoking cessation aid. *Neuropharmacology*. 2007;52:985–94.
24. Nichols AL, Blumenfeld Z, Fan C, Luebbert L, Blom AEM, Cohen BN, et al. Fluorescence activation mechanism and imaging of drug permeation with new sensors for smoking-cessation ligands. *eLife*. 2022;11:e74648.
25. Lipinski CA, Lombardo F, Dominy BW, Feeney PJ. Experimental and computational approaches to estimate solubility and permeability in drug discovery and development settings. *Adv Drug Deliv Rev*. 1997;23:3–25.
26. Bhal SK, Kassam K, Peirson IG, Pearl GM. The rule of five revisited: applying log D in place of log P in drug-likeness filters. *Mol Pharm*. 2007;4:556–60.
27. Smith D, Allerton C, Kalgutkar A, van de Waterbeemd H, Walker D. *Pharmacokinetics and Metabolism in Drug Design*. 3rd ed. Weinheim: Wiley; 2012.
28. Mansoor AMN StatPearls [Internet]. <https://www.ncbi.nlm.nih.gov/books/NBK545280/2022>.
29. Watson PE, Watson ID, Batt RD. Total body water volumes for adult males and females estimated from simple anthropometric measurements. *Am J Clin Nutr*. 1980;33:27–39.
30. Rodgers T, Leahy D, Rowland M. Physiologically based pharmacokinetic modeling 1: predicting the tissue distribution of moderate-to-strong bases. *J Pharm Sci*. 2005;94:1259–76.
31. Ducharme J, Farinotti R. Clinical pharmacokinetics and metabolism of chloroquine. Focus on recent advancements. *Clin Pharmacokinet*. 1996;31:257–74.
32. Shen Q, Wang L, Zhou H, Jiang HD, Yu LS, Zeng S. Stereoselective binding of chiral drugs to plasma proteins. *Acta Pharm Sin*. 2013;34:998–1006.
33. Chuang VT, Otagiri M. Stereoselective binding of human serum albumin. *Chirality*. 2006;18:159–66.
34. Mitchell P. Chemiosmotic coupling in oxidative and photosynthetic phosphorylation. *Biol Rev*. 1966;41:445–502.
35. de Duve C, de Barsey T, Poole B, Trouet A, Tulken P, Van Hoof F. Commentary. Lysosomotropic agents. *Biochem Pharm*. 1974;23:2495–531.
36. Mateus A, Matsson P, Artursson P. Rapid measurement of intracellular unbound drug concentrations. *Mol Pharm*. 2013;10:2467–78.
37. Mateus A, Matsson P, Artursson P. A high-throughput cell-based method to predict the unbound drug fraction in the brain. *J Med Chem*. 2014;57:3005–10.
38. Mateus A, Treyer A, Wegler C, Karlgren M, Matsson P, Artursson P. Intracellular drug bioavailability: a new predictor of system dependent drug disposition. *Sci Rep*. 2017;7:43047.
39. Treyer A, Mateus A, Wisniewski JR, Boriss H, Matsson P, Artursson P. Intracellular drug bioavailability: effect of neutral lipids and phospholipids. *Mol Pharm*. 2018;15:2224–33.
40. Treyer A, Walday S, Boriss H, Matsson P, Artursson P. A cell-free approach based on phospholipid characterization for determination of the cell specific unbound drug fraction (fu,cell). *Pharm Res*. 2019;36:178.
41. Bera K, Kamajaya A, Shivange AV, Muthusamy AK, Nichols AL, Borden PM, et al. Biosensors show the pharmacokinetics of S-ketamine in the endoplasmic reticulum. *Front Cell Neurosci*. 2019;13:499.
42. Muthusamy AK, Kim CH, Virgil SC, Knox HJ, Marvin JS, Nichols AL, et al. Three mutations convert the selectivity of a protein sensor from nicotinic agonists to S-methadone for use in cells, organelles, and biofluids. *J Am Chem Soc*. 2022;144:8480–6.
43. Beatty ZG, Muthusamy AK, Unger EK, Dougherty DA, Tian L, Looger LL, et al. Fluorescence screens for identifying central nervous system-acting drug-biosensor pairs for subcellular and supracellular pharmacokinetics. *Bio Protoc*. 2022;12:e4551.
44. Kapoor R, Peyser TA, Koeppe RE 2nd, Andersen OS. Antidepressants are modifiers of lipid bilayer properties. *J Gen Physiol*. 2019;151:342–56.
45. Yeslevskyy S, Rivel T, Ramseyer C. Curvature increases permeability of the plasma membrane for ions, water and the anti-cancer drugs cisplatin and gemcitabine. *Sci Rep*. 2019;9:17214.
46. Frallicciardi J, Melcr J, Siginou P, Marrink SJ, Poolman B. Membrane thickness, lipid phase and sterol type are determining factors in the permeability of membranes to small solutes. *Nat Commun*. 2022;13:1605.
47. Alves AC, Magarkar A, Horta M, Lima J, Bunker A, Nunes C, et al. Influence of doxorubicin on model cell membrane properties: insights from in vitro and in silico studies. *Sci Rep*. 2017;7:6343.
48. Wray NH, Schappi JM, Singh H, Senese NB, Rasenick MM. NMDAR-independent, cAMP-dependent antidepressant actions of ketamine. *Mol Psychiatry*. 2019;24:1833–43.
49. Sassone-Corsi P. The cyclic AMP pathway. *Cold Spring Harb Perspect Biol*. 2012;4:a011148.
50. Donati RJ, Dwivedi Y, Roberts RC, Conley RR, Pandey GN, Rasenick MM. Post-mortem brain tissue of depressed suicides reveals increased Gs  $\alpha$  localization in lipid raft domains where it is less likely to activate adenylyl cyclase. *J Neurosci*. 2008;28:3042–50.
51. Allen JA, Yu JZ, Dave RH, Bhatnagar A, Roth BL, Rasenick MM. Caveolin-1 and lipid microdomains regulate G<sub>s</sub> trafficking and attenuate G<sub>s</sub> cyclase signaling. *Mol Pharmacol*. 2009;76:1082.
52. Toki S, Donati RJ, Rasenick MM. Treatment of C6 glioma cells and rats with antidepressant drugs increases the detergent extraction of G<sub>s</sub> from plasma membrane. *J Neurochem*. 1999;73:1114–20.
53. Cysz AH, Schappi JM, Rasenick MM. Lateral diffusion of G<sub>s</sub> in the plasma membrane is decreased after chronic but not acute antidepressant treatment: role of lipid raft and non-raft membrane microdomains. *Neuropsychopharmacology*. 2015;40:766–73.
54. Zhang L, Rasenick MM. Chronic treatment with escitalopram but not R-citalopram translocates Galpha(s) from lipid raft domains and potentiates adenylyl cyclase: a 5-hydroxytryptamine transporter-independent action of this antidepressant compound. *J Pharm Exp Ther*. 2010;332:977–84.
55. Erb SJ, Schappi JM, Rasenick MM. Antidepressants accumulate in lipid rafts independent of monoamine transporters to modulate redistribution of the G protein, G<sub>s</sub>. *J Biol Chem*. 2016;291:19725–33.
56. Nichols AL, Blumenfeld Z, Luebbert L, Knox HJ, Muthusamy AK, Marvin JS, et al. Selective serotonin reuptake inhibitors within cells: temporal resolution in cytoplasm, endoplasmic reticulum, and membrane. *J Neurosci*. 2023;43:2222–41.
57. Casarotto PC, Giry M, Fred SM, Kovaleva V, Moliner R, Enkavi G, et al. Antidepressant drugs act by directly binding to TRKB neurotrophin receptors. *Cell*. 2021;184:1299–313.e19.
58. Hille B. Local anesthetics: hydrophilic and hydrophobic pathways for the drug-receptor reaction. *J Gen Physiol*. 1977;69:497–515.
59. Smith DA, Rowland M. Intracellular and intraorgan concentrations of small molecule drugs: theory, uncertainties in infectious diseases and oncology, and promise. *Drug Metab Dispos*. 2019;47:665–72.
60. Hille B. The pH-dependent rate of action of local anesthetics on the node of Ranvier. *J Gen Physiol*. 1977;69:475–96.
61. Tischbirek CH, Wenzel EM, Zheng F, Huth T, Amato D, Trapp S, et al. Use-dependent inhibition of synaptic transmission by the secretion of intravesicularly accumulated antipsychotic drugs. *Neuron*. 2012;74:830–44.
62. Hay T, Jones R, Beaumont K, Kemp M. Modulation of the partition coefficient between octanol and buffer at pH 7.4 and pKa to achieve the optimum balance of blood clearance and volume of distribution for a series of tetrahydropyran histamine type 3 receptor antagonists. *Drug Metab Dispos*. 2009;37:1864–70.
63. Lu S, Sung T, Lin N, Abraham RT, Jessen BA. Lysosomal adaptation: how cells respond to lysosomotropic compounds. *PLoS ONE*. 2017;12:e0173771.

64. Fu D, Zhou J, Zhu WS, Manley PW, Wang YK, Hood T, et al. Imaging the intracellular distribution of tyrosine kinase inhibitors in living cells with quantitative hyperspectral stimulated Raman scattering. *Nat Chem*. 2014;6:614–22.
65. Lenz B, Brink A, Mihatsch MJ, Altmann B, Niederhauser U, Steinhuber B, et al. Multiorgan crystal deposition of an amphoteric drug in rats due to lysosomal accumulation and conversion to a poorly soluble hydrochloride salt. *Toxicol Sci*. 2021;180:383–94.
66. Lester HA, Xiao C, Srinivasan R, Son C, Miwa J, Pantoja R, et al. Nicotine is a selective pharmacological chaperone of acetylcholine receptor number and stoichiometry. implications for drug discovery. *AAPS J*. 2009;11:167–77.
67. Govind AP, Vallejo YF, Stolz JR, Yan JZ, Swanson GT, Green WN. Selective and regulated trapping of nicotinic receptor weak base ligands and relevance to smoking cessation. *eLife*. 2017;6:e25651.
68. Tucker KR, Block ER, Levitan ES. Action potentials and amphetamine release antipsychotic drug from dopamine neuron synaptic VMAT vesicles. *Proc Natl Acad Sci USA*. 2015;112:E4485–94.
69. Duvvuri M, Gong Y, Chatterji D, Krise JP. Weak base permeability characteristics influence the intracellular sequestration site in the multidrug-resistant human leukemic cell line HL-60. *J Biol Chem*. 2004;279:32367–72.
70. Trapp S, Rosania GR, Horobin RW, Kornhuber J. Quantitative modeling of selective lysosomal targeting for drug design. *Eur Biophys J*. 2008;37:1317–28.
71. Abdel-Razaq W, Kendall DA, Bates TE. The effects of antidepressants on mitochondrial function in a model cell system and isolated mitochondria. *Neurochem Res*. 2011;36:327–38.
72. de Oliveira MR. Fluoxetine and the mitochondria: a review of the toxicological aspects. *Toxicol Lett*. 2016;258:185–91.
73. Shaner NC, Campbell RE, Steinbach PA, Giepmans BN, Palmer AE, Tsien RY. Improved monomeric red, orange and yellow fluorescent proteins derived from *Discosoma* sp. red fluorescent protein. *Nat Biotechnol*. 2004;22:1567–72.
74. Koveal D, Rosen PC, Meyer DJ, Diaz-Garcia CM, Wang Y, Cai LH, et al. A high-throughput multiparameter screen for accelerated development and optimization of soluble genetically encoded fluorescent biosensors. *Nat Commun*. 2022;13:2919.
75. Patriarchi T, Cho JR, Merten K, Howe MW, Marley A, Xiong WH, et al. Ultrafast neuronal imaging of dopamine dynamics with designed genetically encoded sensors. *Science*. 2018;360:eaat4422.
76. Jing M, Zhang P, Wang G, Feng J, Mesik L, Zeng J, et al. A genetically encoded fluorescent acetylcholine indicator for in vitro and in vivo studies. *Nat Biotechnol*. 2018;36:726–37.
77. Runge K, Cardoso C, de Chevigny A. Dendritic spine plasticity: function and mechanisms. *Front Synaptic Neurosci*. 2020;12:36.
78. Ren Z, Pribragh H, Jefferson SJ, Shorey M, Fuchs T, Stellwagen D, et al. Bidirectional homeostatic regulation of a depression-related brain state by gamma-aminobutyric acidergic deficits and ketamine treatment. *Biol Psychiatry*. 2016;80:457–68.
79. Moda-Sava RN, Murdock MH, Parekh PK, Fetcho RN, Huang BS, Huynh TN, et al. Sustained rescue of prefrontal circuit dysfunction by antidepressant-induced spine formation. *Science*. 2019;364:eaat8078.
80. Ly C, Greb AC, Vargas MV, Duim WC, Grodzki ACG, Lein PJ, et al. Transient stimulation with psychoplastogens is sufficient to initiate neuronal growth. *ACS Pharm Transl Sci*. 2021;4:452–60.
81. Reines A, Cereseto M, Ferrero A, Sifonios L, Podestá MF, Wikinski S. Maintenance treatment with fluoxetine is necessary to sustain normal levels of synaptic markers in an experimental model of depression: correlation with behavioral response. *Neuropsychopharmacology*. 2008;33:1896–908.
82. Cameron LP, Tombari RJ, Lu J, Pell AJ, Hurley ZQ, Ehinger Y, et al. A non-hallucinogenic psychedelic analogue with therapeutic potential. *Nature*. 2021;589:474–79.
83. Park D, Wu Y, Wang X, Gowrishankar S, Baublis A, De, et al. Synaptic vesicle proteins and ATG9A self-organize in distinct vesicle phases within synapsin condensates. *Nat Commun*. 2023;14:455.
84. Chen X, Jia B, Zhu S, Zhang M. Phase separation-mediated actin bundling by the postsynaptic density condensates. *eLife*. 2023;12:e84446.
85. Xing G, Jing H, Yu Z, Chen P, Wang H, Xiong WC, et al. Membraneless condensates by Rapsn phase separation as a platform for neuromuscular junction formation. *Neuron*. 2021;109:1963–78.e5.
86. Jain A, Vale RD. RNA phase transitions in repeat expansion disorders. *Nature*. 2017;546:243–47.
87. Alberti S, Dormann D. Liquid-liquid phase separation in disease. *Annu Rev Genet*. 2019;53:171–94.
88. Pezzotti S, König B, Ramos S, Schwaab G, Havenith M. Liquid-liquid phase separation? ask the water! *J Phys Chem Lett*. 2023;14:1556–63.
89. Chong C, Schug SA, Page-Sharp M, Jenkins B, Ilett KF. Development of a sublingual/oral formulation of ketamine for use in neuropathic pain: preliminary findings from a three-way randomized, crossover study. *Clin Drug Investig*. 2009;29:317–24.
90. Kharasch ED, Labroo R. Metabolism of ketamine stereoisomers by human liver microsomes. *Anesthesiology*. 1992;77:1201–7.
91. Yanagihara Y, Kariya S, Ohtani M, Uchino K, Aoyama T, Yamamura Y, et al. Involvement of CYP2B6 in n-demethylation of ketamine in human liver microsomes. *Drug Metab Dispos*. 2001;29:887–90.
92. Hijazi Y, Bouliou R. Contribution of CYP3A4, CYP2B6, and CYP2C9 isoforms to N-demethylation of ketamine in human liver microsomes. *Drug Metab Dispos*. 2002;30:853–8.
93. Yanagihara Y, Ohtani M, Kariya S, Uchino K, Hiraishi T, Ashizawa N, et al. Plasma concentration profiles of ketamine and norketamine after administration of various ketamine preparations to healthy Japanese volunteers. *Biopharm Drug Dispos*. 2003;24:37–43.
94. Desta Z, Moaddel R, Ogburn ET, Xu C, Ramamoorthy A, Venkata SL, et al. Stereoselective and regio-specific hydroxylation of ketamine and norketamine. *Xenobiotica*. 2012;42:1076–87.
95. Zhao X, Venkata SL, Moaddel R, Luckenbaugh DA, Brutsche NE, Ibrahim L, et al. Simultaneous population pharmacokinetic modelling of ketamine and three major metabolites in patients with treatment-resistant bipolar depression. *Br J Clin Pharm*. 2012;74:304–14.
96. Zanos P, Moaddel R, Morris PJ, Riggs LM, Highland JN, Georgiou P, et al. Ketamine and ketamine metabolite pharmacology: insights into therapeutic mechanisms. *Pharm Rev*. 2018;70:621–60.
97. Ebert B, Mikkelsen S, Thorkildsen C, Borgbjerg FM. Norketamine, the main metabolite of ketamine, is a non-competitive NMDA receptor antagonist in the rat cortex and spinal cord. *Eur J Pharmacol*. 1997;333:99–104.
98. Moaddel R, Abdrakhmanova G, Kozak J, Jozwiak K, Toll L, Jimenez L, et al. Sub-anesthetic concentrations of (R,S)-ketamine metabolites inhibit acetylcholine-evoked currents in  $\alpha 7$  nicotinic acetylcholine receptors. *Eur J Pharmacol*. 2013;698:228–34.
99. Oye I, Paulsen O, Maurset A. Effects of ketamine on sensory perception: evidence for a role of N-methyl-D-aspartate receptors. *J Pharm Exp Ther*. 1992;260:1209–13.
100. White Paul F, Ham J, Way Walter L, Trevor A. Pharmacology of ketamine isomers in surgical patients. *Anesthesiology*. 1980;52:231–39.
101. White PF, Schöttler J, Shafer A, Stanski DR, Horai Y, Trevor AJ. Comparative pharmacology of the ketamine isomers. Studies in volunteers. *Br J Anaesth*. 1985;57:197–203.
102. Mathisen LC, Skjelbred P, Skoglund LA, Øye I. Effect of ketamine, an NMDA receptor inhibitor, in acute and chronic orofacial pain. *Pain*. 1995;61:215–20.
103. Vollenweider FX, Leenders KL, Oye I, Hell D, Angst J. Differential psychopathology and patterns of cerebral glucose utilisation produced by (S)- and (R)-ketamine in healthy volunteers using positron emission tomography (PET). *Eur Neuropsychopharmacol*. 1997;7:25–38.
104. Highland JN, Morris PJ, Zanos P, Lovett J, Ghosh S, Wang AQ, et al. Mouse, rat, and dog bioavailability and mouse oral antidepressant efficacy of (2R,6R)-hydroxynorketamine. *J Psychopharmacol*. 2019;33:12–24.
105. Geisslinger G, Hering W, Thomann P, Knoll R, Kamp HD, Brune K. Pharmacokinetics and pharmacodynamics of ketamine enantiomers in surgical patients using a stereoselective analytical method. *Br J Anaesth*. 1993;70:666–71.
106. Zarate CA Jr., Brutsche N, Laje G, Luckenbaugh DA, Venkata SL, Ramamoorthy A, et al. Relationship of ketamine's plasma metabolites with response, diagnosis, and side effects in major depression. *Biol Psychiatry*. 2012;72:331–8.
107. Loo CK, Gálvez V, O'Keefe E, Mitchell PB, Hadzi-Pavlovic D, Leyden J, et al. Placebo-controlled pilot trial testing dose titration and intravenous, intramuscular and subcutaneous routes for ketamine in depression. *Acta Psychiatr Scand*. 2016;134:48–56.
108. Clements JA, Nimmo WS, Grant IS. Bioavailability, pharmacokinetics, and analgesic activity of ketamine in humans. *J Pharm Sci*. 1982;71:539–42.
109. Lapidus KA, Levitch CF, Perez AM, Brallier JW, Parides MK, Soleimani L, et al. A randomized controlled trial of intranasal ketamine in major depressive disorder. *Biol Psychiatry*. 2014;76:970–6.
110. Canuso CM, Singh JB, Fedgchin M, Alphas L, Lane R, Lim P, et al. Efficacy and safety of intranasal esketamine for the rapid reduction of symptoms of depression and suicidality in patients at imminent risk for suicide: results of a double-blind, randomized, placebo-controlled study. *Am J psychiatry*. 2018;175:620–30.
111. Daly EJ, Trivedi MH, Janik A, Li H, Zhang Y, Li X, et al. Efficacy of esketamine nasal spray plus oral antidepressant treatment for relapse prevention in patients with treatment-resistant depression: a randomized clinical trial. *JAMA Psychiatry*. 2019;76:893–903.
112. Popova V, Daly EJ, Trivedi M, Cooper K, Lane R, Lim P, et al. Efficacy and safety of flexibly dosed esketamine nasal spray combined with a newly initiated oral antidepressant in treatment-resistant depression: a randomized double-blind active-controlled study. *Am J psychiatry*. 2019;176:428–38.



113. Jeon HJ, Ju PC, Sulaiman AH, Aziz SA, Paik JW, Tan W, et al. Long-term safety and efficacy of esketamine nasal spray plus an oral antidepressant in patients with treatment-resistant depression- an asian sub-group analysis from the SUSTAIN-2 study. *Clin Psychopharmacol Neurosci*. 2022;20:70–86.
114. Anand A, Mathew SJ, Sanacora G, Murrrough JW, Goes FS, Altinay M, et al. Ketamine versus ECT for nonpsychotic treatment-resistant major depression. *N Engl J Med*. 2023;388:2315–25.
115. McIntyre RS, Carvalho IP, Lui LMW, Majeed A, Masand PS, Gill H, et al. The effect of intravenous, intranasal, and oral ketamine in mood disorders: a meta-analysis. *J Affect Disord*. 2020;276:576–84.
116. Leal GC, Bandeira ID, Correia-Melo FS, Telles M, Mello RP, Vieira F, et al. Intravenous arketamine for treatment-resistant depression: open-label pilot study. *Eur Arch Psychiatry Clin Neurosci*. 2021;271:577–82.
117. Clinical\_Trials\_Data\_Base. A randomized, placebo-controlled, double-blind study to assess safety and efficacy of PCN-101 in TRD. <https://ClinicalTrials.gov/show/NCT05414422>.
118. Dinis-Oliveira RJ. Metabolism and metabolomics of ketamine: a toxicological approach. *Forensic Sci Res*. 2017;2:2–10.
119. Moaddel R, Venkata SL, Tanga MJ, Bupp JE, Green CE, Iyer L, et al. A parallel chiral-achiral liquid chromatographic method for the determination of the stereoisomers of ketamine and ketamine metabolites in the plasma and urine of patients with complex regional pain syndrome. *Talanta*. 2010;82:1892–904.
120. Cohen ML, Chan SL, Way WL, Trevor AJ. Distribution in the brain and metabolism of ketamine in the rat after intravenous administration. *Anesthesiology*. 1973;39:370–6.
121. Leung LY, Baillie TA. Comparative pharmacology in the rat of ketamine and its two principal metabolites, norketamine and (Z)-6-hydroxynorketamine. *J Med Chem*. 1986;29:2396–9.
122. Paul RK, Singh NS, Khadeer M, Moaddel R, Sanghvi M, Green CE, et al. (R,S)-Ketamine metabolites (R,S)-norketamine and (2S,6S)-hydroxynorketamine increase the mammalian target of rapamycin function. *Anesthesiology*. 2014;121:149–59.
123. Moaddel R, Sanghvi M, Dossou KS, Ramamoorthy A, Green C, Bupp J, et al. The distribution and clearance of (2S,6S)-hydroxynorketamine, an active ketamine metabolite, in Wistar rats. *Pharm Res Perspect*. 2015;3:e00157.
124. Zanos P, Moaddel R, Morris PJ, Georgiou P, Fischell J, Elmer GI, et al. NMDAR inhibition-independent antidepressant actions of ketamine metabolites. *Nature*. 2016;533:481–6.
125. Bonaventura J, Gomez JL, Carlton ML, Lam S, Sanchez-Soto M, Morris PJ, et al. Target deconvolution studies of (2R,6R)-hydroxynorketamine: an elusive search. *Mol Psychiatry*. 2022;27:4144–56.
126. Corazza O, Schifano F, Simonato P, Fergus S, Assi S, Stair J, et al. Phenomenon of new drugs on the Internet: the case of ketamine derivative methoxetamine. *Hum Psychopharmacol*. 2012;27:145–9.
127. Hofer KE, Grager B, Müller DM, Rauber-Lüthy C, Kupferschmidt H, Rentsch KM, et al. Ketamine-like effects after recreational use of methoxetamine. *Ann Emerg Med*. 2012;60:97–9.
128. Kjellgren A, Jonsson K. Methoxetamine (MXE)-a phenomenological study of experiences induced by a “legal high” from the internet. *J Psychoact Drugs*. 2013;45:276–86.
129. Striebel JM, Nelson EE, Kalapatapu RK. “Being with a buddha”: a case report of methoxetamine use in a united states veteran with PTSD. *Case Rep Psychiatry*. 2017;2017:2319094.
130. Morris H, Wallach J. From PCP to MXE: a comprehensive review of the non-medical use of dissociative drugs. *Drug Test Anal*. 2014;6:614–32.
131. Horsley RR, Lhotkova E, Hajkova K, Jurasek B, Kuchar M, Palenicek T. Detailed pharmacological evaluation of methoxetamine (MXE), a novel psychoactive ketamine analogue—behavioural, pharmacokinetic and metabolic studies in the Wistar rat. *Brain Res Bull*. 2016;126:102–10.
132. Roth BL, Gibbons S, Arunotayanun W, Huang XP, Setola V, Treble R, et al. The ketamine analogue methoxetamine and 3- and 4-methoxy analogues of phencyclidine are high affinity and selective ligands for the glutamate NMDA receptor. *PLoS ONE*. 2013;8:e59334.
133. Hondebrink L, Kasteel EEJ, Tukker AM, Wijnolts FMJ, Verboven AHA, Westerink RHS. Neuropharmacological characterization of the new psychoactive substance methoxetamine. *Neuropharmacology*. 2017;123:1–9.
134. Chiamulera C, Armani F, Mutti A, Fattore L. The ketamine analogue methoxetamine generalizes to ketamine discriminative stimulus in rats. *Behav Pharm*. 2016;27:204–10.
135. Zanda MT, Fadda P, Antinori S, Di Chio M, Fratta W, Chiamulera C, et al. Methoxetamine affects brain processing involved in emotional response in rats. *Br J Pharm*. 2017;174:3333–45.
136. Páleníček T, Fujáková M, Brunovský M, Balíková M, Horáček J, Gorman I, et al. Electroencephalographic spectral and coherence analysis of ketamine in rats: correlation with behavioral effects and pharmacokinetics. *Neuropsychobiology*. 2011;63:202–18.
137. Renner UD, Oertel R, Kirch W. Pharmacokinetics and pharmacodynamics in clinical use of scopolamine. *Ther Drug Monit*. 2005;27:655–65.
138. Damaj MI, Carroll FI, Eaton JB, Navarro HA, Blough BE, Mirza S, et al. Enantio-selective effects of hydroxy metabolites of bupropion on behavior and on function of monoamine transporters and nicotinic receptors. *Mol Pharm*. 2004;66:675–82.
139. Goodwin GM, Aaronson ST, Alvarez O, Arden PC, Baker A, Bennett JC, et al. Single-dose psilocybin for a treatment-resistant episode of major depression. *N Engl J Med*. 2022;387:1637–48.
140. Vollenweider FX, Preller KH. Psychedelic drugs: neurobiology and potential for treatment of psychiatric disorders. *Nat Rev Neurosci*. 2020;21:611–24.
141. Hesselgrave N, Troppoli TA, Wulff AB, Cole AB, Thompson SM. Harnessing psilocybin: antidepressant-like behavioral and synaptic actions of psilocybin are independent of 5-HT<sub>2R</sub> activation in mice. *Proc Natl Acad Sci USA*. 2021;118:e2022489118.

## AUTHOR CONTRIBUTIONS

All authors wrote and edited all portions of the manuscript. KB provided final formatting of Table 1 and the Supplementary Files and also conceived the Figures.

## FUNDING

The group of HAL has been funded by the National Institute of Mental Health (MH1230823), the National Institute of General Medical Science (GM123582), National Institute on Drug Abuse (DA043829, DA049140), and the California Tobacco-Related Disease Research Program (27IP-0057). KB was supported by the Della Martin Foundation and the Howard Hughes Medical Institute. The group of EC was supported by the Academy of Finland (294710, 303124, 307416 and 327192), Sigríd Jusélius Foundation, and Jane and Aatos Erkko Foundation.

## COMPETING INTERESTS

The authors declare no competing interests.

## ADDITIONAL INFORMATION

**Supplementary information** The online version contains supplementary material available at <https://doi.org/10.1038/s41386-023-01725-x>.

**Correspondence** and requests for materials should be addressed to Henry A. Lester.

**Reprints and permission information** is available at <http://www.nature.com/reprints>

**Publisher's note** Springer Nature remains neutral with regard to jurisdictional claims in published maps and institutional affiliations.

Springer Nature or its licensor (e.g. a society or other partner) holds exclusive rights to this article under a publishing agreement with the author(s) or other rightsholder(s); author self-archiving of the accepted manuscript version of this article is solely governed by the terms of such publishing agreement and applicable law.